Thermodynamic Analysis of an Antibody Functional Epitope

Robert F. Kelley* and Mark P. O'Connell

Protein Engineering Department, Genentech, Inc., 460 Point San Bruno Boulevard, South San Francisco, California 94080

Received January 25, 1993; Revised Manuscript Received April 29, 1993

ABSTRACT: We have probed the relative contribution of polar and nonpolar interactions to antibody–antigen interaction by measuring the effect of single amino acid substitutions in an humanized anti-p185^{HER2} antibody (hu4D5-5) on the thermodynamics of antigen binding. First we mapped the functional epitope by complete alanine-scan mutagenesis of the antibody complementarity-determining region (CDR). Four residues, H91 in V_L and R50, W95, and Y100a in V_H, make large contributions to the free energy of binding ($\Delta\Delta G > 3$ kcal mol^{-1}) and have $\Delta\Delta G > \Delta\Delta H$. These residues are clustered in a shallow pocket on the antibody surface in the X-ray structure determined for hu4D5 Fv. The majority of other CDR residues make less energetically important contributions ($\Delta\Delta G < 1$ kcal mol^{-1}) to binding but have $\Delta\Delta H > \Delta\Delta G$, suggesting that the wild-type side chain does contact antigen but the loss in entropy, perhaps through restriction of side-chain conformational freedom, offsets the favorable enthalpic term. Effects of Phe and Ala substitutions on the ΔG and ΔC_p of antigen binding indicate that the favorable contribution of antibody tyrosine residues to binding results primarily from burial of the aromatic ring in the interface with antigen. Burial of the phenyl ring has a favorable ΔH at 25 °C but at least for one site (V_L-Y92) is opposed by ΔS. This latter feature is inconsistent with the thermodynamics predicted for the hydrophobic effect based on hydrocarbon-transfer experiments. In addition, the magnitude of ΔC_p for burial of the phenyl ring is greater than would be predicted from the model compound data. These results suggest that the aromatic ring of antibody Tyr residues may contribute other interactions to antigen binding, such as aromatic hydrogen bonding, in addition to the contribution from the hydrophobic effect.

A quantitative understanding of both protein folding and protein–protein interaction requires accurate structural and thermodynamic information. Predictions about the thermodynamics of the fundamental forces involved, which are primarily electrostatic interactions (including hydrogen bonding) and the hydrophobic effect, usually originate from studies of small, model compounds which may not be representative of macromolecular systems. For example, the thermodynamic parameters governing the hydrophobic effect (Kauzmann, 1959; Tanford, 1980), which is presumed to arise from the ordering of water around nonpolar groups, have been extracted from studies of the transfer of liquid hydrocarbons to water (Gill et al., 1976) and more recently from measurements on the aqueous dissolution of solid compounds (Murphy & Gill, 1991). Although neither model accurately depicts burial of an amino acid side chain in the protein interior or interface, results of both liquid hydrocarbon transfer and solid dissolution experiments suggest that polar and nonpolar interactions differ in the sign of the change in heat capacity (ΔC_p). Transfer of polar and nonpolar groups from water to a less polar environment has positive and negative contributions to ΔC_p, respectively. Therefore, mutations that weaken the hydrophobic contribution to folding or association should make ΔC_p less negative (positive $\Delta\Delta C_p$) whereas decreasing polar interactions should make ΔC_p more negative (negative $\Delta\Delta C_p$).

We have chosen to test the predictions of the model compound studies by determining the thermodynamic consequences for antigen binding of alanine substitutions (Cunningham & Wells, 1989) in the CDR[1] loops of an antibody. Available X-ray structures (Davies et al., 1990) indicate that most of the antigen contact residues are provided by the six CDR loops of an antibody, three from the light chain variable domain (V_L) and three from the heavy chain variable domain (V_H). Upon complex formation with protein antigen, antibodies lose 690–886 Å^2 of accessible surface, with 14–21 residues in contact with antigen. Antigen binding involves formation of 10–23 hydrogen bonds and 0–3 salt links (Davies et al., 1990). These values are similar to other protein–protein interactions. Nonetheless, free energy calculations (Novotny et al., 1989) suggest that only a subset of these contacts actively contributes to the free energy of binding. Antibody CDR loops are rich in tyrosine residues (Padlan, 1990) which could participate in antigen binding through side-chain hydrogen bonds or by burial of the nonpolar aromatic ring. These roles can be distinguished by thermodynamic measurements on mutant proteins.

The murine monoclonal antibody 4D5 (Hudziak et al., 1989) was raised against the extracellular domain of human epidermal growth factor receptor 2 and has been "humanized" (Riechmann et al., 1988) by Carter et al. (1992b) for testing as an anticancer agent. X-ray structures have been determined for both Fab and Fv fragments of the humanized antibody (Eigenbrot et al., 1993), but a structure of the complex with antigen is not yet available. We describe here results of experiments aimed at determining the antibody CDR residues important for antigen binding. Binding constants for the interaction of mutated Fab fragments with antigen were determined from kinetic experiments by using SPR methods (Karlsson et al., 1991); enthalpy (ΔH) and heat capacity changes (ΔC_p) were measured by using isothermal titration calorimetry (Langerman & Biltonen, 1979; Wiseman et al.,

[1] Abbreviations: p185^{HER2}, human epidermal growth factor receptor 2 (also called *c-erbB*-2); p185$^{HER2-ECD}$, extracellular domain of p185^{HER2}; CDR, complementarity-determining region; SPR, surface plasmon resonance; RIA, radioimmunoassay; hu, humanized. Mutants are named with the prefix denoting the light chain (V_L) or heavy chain (V_H) variable domain, followed by the single-letter code for the residue found in the wild-type antibody (hu4D5-5), then the sequence position, and the residue in the mutant. Double mutants are designated with a colon separating the two amino acid changes. Residue numbering is according to Kabat et al. (1991).

0006-2960/93/0432-6828$04.00/0

1989; Kelley et al., 1992). We find that a few CDR residues dominate the ΔG of antigen binding, but ΔH measurements suggest many more residues contact antigen.

EXPERIMENTAL PROCEDURES

Production of hu4D5-5 Mutants. Solvent-accessible CDR residues were initially selected for mutagenesis on the basis of an examination of a model (Carter et al., 1992b) of hu4D5-5 Fv. X-ray structures for both Fab and Fv fragments of humanized 4D5 have been recently determined and confirm most of the salient features of the model (Eigenbrot et al., 1993). Alanine substitution mutants of hu4D5-5 Fab ("wild-type") were constructed by using cassette mutagenesis (Wells et al., 1985), expressed at high levels (0.5–2.0 g/L) by secretion from *Escherichia coli* (Carter et al., 1992a) and purified as described previously (Kelley et al., 1992). Alanine mutants V_L-D28A and V_L-F53A expressed very poorly, and thus the antigen binding contribution of these sites was probed by Asn substitutions. All of the purified mutant proteins gave nearly identical far-UV–CD spectra (data not shown), indicating that the mutation does not significantly perturb the immunoglobulin fold. The extracellular domain of $p185^{HER2}$ is a 624 amino acid polypeptide produced by recombinant expression in CHO cells and purified as described previously (Fendly et al., 1990).

Determination of the K_D for Antigen Binding. Binding constants for the interaction of hu4D5 Fab fragments with the receptor extracellular domain ($p185^{HER2\text{-}ECD}$) were determined by using the method of surface plasmon resonance (SPR) (Karlsson et al., 1991) on a Pharmacia Biacore system. In this method, the binding constant is determined from the ratio of kinetic constants for dissociation and association of antibody from immobilized antigen.

$$K_D = k_{diss}/k_{assoc} \quad (1)$$

Antigen is immobilized in a dextran layer over a gold film on a sensor chip by covalent coupling through free amino groups. A flow system is used to introduce reactants. Binding of antibody is observed by changes in refractive index (R), and thus no labeling of components is required. Binding reactions are run under pseudo-first-order conditions with the kinetics of binding related to the refractive index changes as

$$dR/dt = \text{constant} - (k_{assoc}C + k_{diss})R \quad (2)$$

where C is the concentration of antibody flowing over the chip surface. A plot of dR/dt versus R will have a slope of $-k_{obs}$ where

$$k_{obs} = k_{assoc}C + k_{diss} \quad (3)$$

The kinetic constants can then be evaluated by determining the concentration dependence of k_{obs} with k_{assoc} given by the slope and k_{diss} by the intercept. Determination of k_{diss} from the intercept usually requires a long extrapolation, and thus a large error, so k_{diss} is normally extracted from the initial rate of dissociation upon return to buffer flow. In this situation, C is 0 and k_{diss} is calculated from

$$\ln(R_t/R_n) = k_{diss}(t_n - t) \quad (4)$$

where R_t is the refractive index at time t and R_n is the refractive index at a reference point t_n along the dissociation curve. This experiment requires saturation of the binding sites in order to minimize the potential for rebinding of the antibody that dissociates. Errors in k_{diss} due to rebinding are also minimized by using only the initial dissociation data to calculate the kinetic constant.

$p185^{HER2\text{-}ECD}$ was immobilized through free amino groups using a protocol supplied by the manufacturer. Antigen was immobilized at a density of approximately 0.02 pmol mm^{-2} which, given the molecular weight of 68 000, corresponds to a refractive index change (RU; arbitrary units) of about 1000. All measurements were performed at ambient temperature using solutions containing 20 mM sodium phosphate, pH 7.5, 0.1 M sodium chloride, and 0.05% Tween-20 at a flow rate of 10 μL min^{-1}. An aliquot (30 μL) of a solution of Fab was injected at about 60 s, with return to buffer flow at about 240 s. In dissociation experiments, the refractive index change was monitored for about 30 min after return to buffer flow before regeneration of the chip by acid elution of any Fab remaining bound (injection of a 15-μL aliquot of 10 mM HCl). Many cycles of binding and regeneration with acid could be performed with no detectable losses in affinity. In association experiments, the signal was monitored for about 2 min after return to buffer flow prior to acid regeneration.

Bimolecular association rate constants (k_{assoc}) were determined from the concentration dependence of the observed rate of association (k_{obs}). A series of concentrations ranging from 15.6 nM to 1 μM in 4-fold increments were commonly employed. Dissociation rate constants (k_{diss}) were determined by saturating immobilized antigen with 20 μM Fab and monitoring dissociation upon return to buffer flow. Two single-site mutants, V_H-W95A and V_H-Y100aA, had dissociation rates that were too fast ($>10^{-2}$ s^{-1}) for determination of k_{diss} from the dissociation phase. In addition, the doubly mutated Fab bound so weakly that saturation could not be achieved even at concentrations as high as 400 μM. The k_{diss} values for these mutants were determined from the intercept of a plot of k_{obs} on concentration and thus have large errors.

Determination of ΔH and ΔC_p for Antigen Binding. Measurements of the enthalpy change (ΔH) associated with hu4D5 Fab binding to $p185^{HER2\text{-}ECD}$ were performed at 25.4 ± 0.2 °C on a Microcal, Inc., OMEGA titration calorimeter as previously described (Kelley et al., 1992). Antibody and antigen were prepared for measurements by extensive dialysis at ambient temperature versus a buffer solution of 20 mM sodium phosphate, pH 7.5, containing 0.1 M NaCl. At the concentrations of antigen used for precise ΔH determination (5–10 μM $p185^{HER2\text{-}ECD}$) the "c" value (Wiseman et al., 1989) for most of the mutant hu4D5 Fab was greater than 10^4, thus precluding a calorimetric measurement of the binding constant. Both V_H-W95A and V_H-Y100aA Fab bound antigen with sufficiently reduced affinity, but still measurable ΔH, such that the binding constant could be determined from calorimetry. For several of the mutant proteins, enthalpy measurements were also made at 37 °C in order to determine ΔC_p from the relationship

$$\Delta C_p = \frac{\Delta H(T_2) - \Delta H(T_1)}{T_2 - T_1} \quad (5)$$

The enthalpy change for binding of hu4D5-5 Fab to $p185^{HER2\text{-}ECD}$ has been previously shown to have a linear dependence on temperature in the range of 25–45 °C (Kelley et al., 1992), and it is assumed that this linear relationship is maintained for the mutant proteins. These temperatures are considerably lower than required for thermal denaturation of hu4D5-5 Fab (T_m = 82 °C; Kelley et al., 1992) or $p185^{HER2\text{-}ECD}$ (T_m = 65 °C; R. Kelley, unpublished results), and thus there is no contribution to the measured ΔC_p from protein folding.

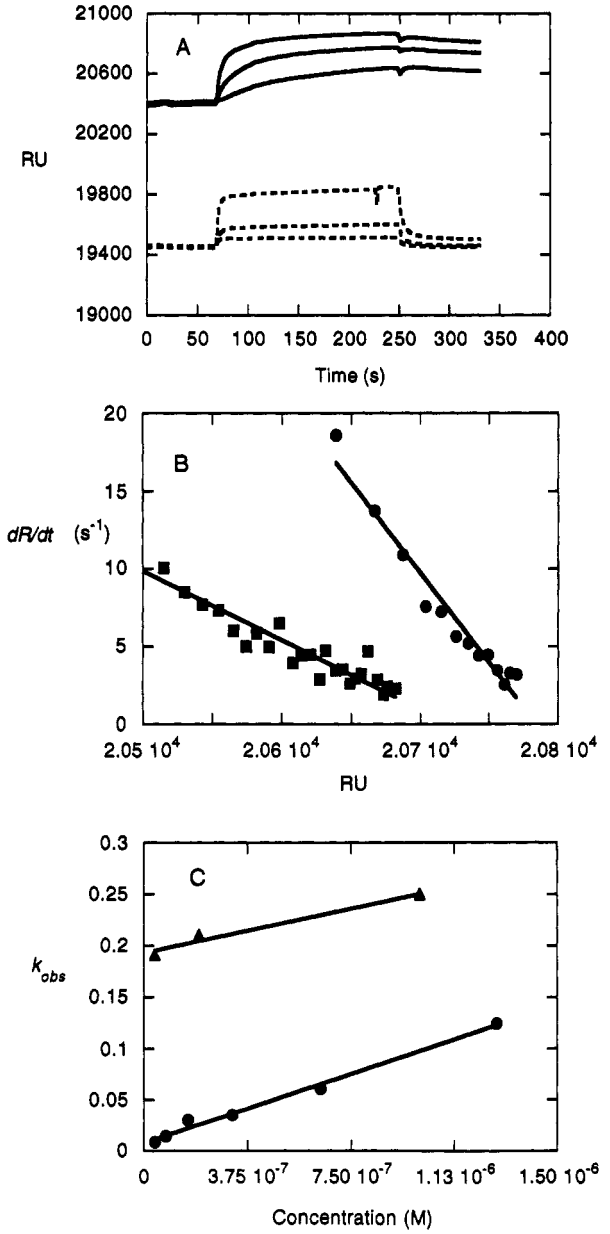

FIGURE 1: Association kinetics for Fab binding to immobilized p185$^{HER2-ECD}$ determined by using SPR. (A) Association curves for hu4D5-5 (solid lines) at 80 nM (bottom curve), 320 nM (middle curve), and 1.28 μM (top curve) as well as curves for V_H-Y100aA (dotted lines) at 40 nM (bottom curve), 200 nM (middle curve), and 1 μM (top curve) are shown (RU, refractive index units). The V_H-Y100aA curves have been offset for clearer display. (B) Illustration of k_{obs} determination by employing eq 2. Data for association of 320 nM (filled squares) and 1.28 μM (filled circles) hu4D5-5 Fab are shown, with the solid lines the result of linear least-squares analysis. (C) Concentration dependence of k_{obs} for hu4D5-5 (filled circles) and V_H-Y100aA (filled triangles) Fab. Solid lines are the result of linear least-squares analysis using eq 3.

RESULTS AND DISCUSSION

Kinetics of Antibody–Antigen Interaction. Typical SPR data for association of hu4D5-5 (wild-type) Fab to immobilized p185$^{HER2-ECD}$ are shown in Figure 1. Both the extent and rate of association, as monitored by changes in refractive index (Figure 1A), increased with increasing Fab concentration. These data were analyzed by using eq 2 as shown in Figure 1B to obtain k_{obs} at each concentration. In the range of 10 nM to 1.3 μM Fab concentration, k_{obs} displayed a linear dependence on concentration (Figure 1C), having a slope (k_{assoc}) of 6.4 ± 0.9 × 10^4 M^{-1} s^{-1}. Below this range, the rate of association was too small to measure, and at higher

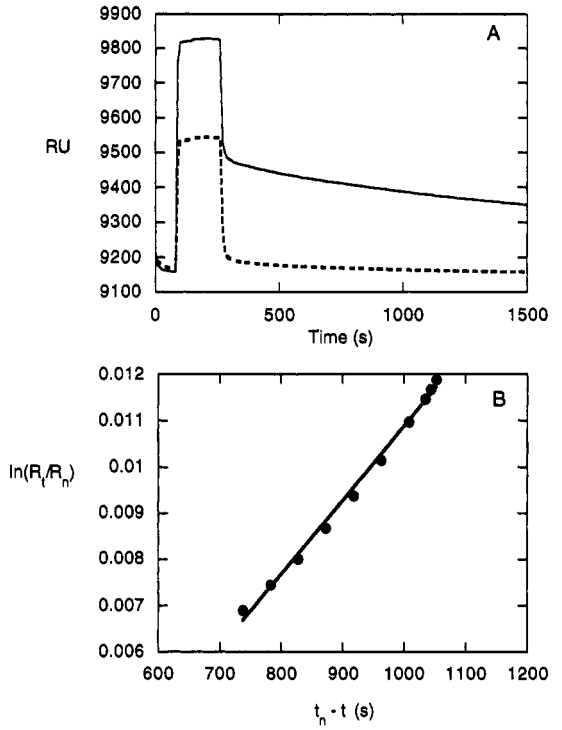

FIGURE 2: Kinetics of dissociation of Fab from immobilized p185$^{HER2-ECD}$ using SPR. (A) SPR profiles observed with 20 μM hu4D5-5 (solid line) or V_H-Y100aA (dashed line) Fab are shown. (B) Analysis of the hu4D5-5 dissociation data using eq 4. A reference point (t_n) of 1400 s was used, and the initial dissociation data (ca. 300–700-s range of panel A) were subjected to linear least-squares analysis (solid line).

concentrations the rate became too fast. By comparison, the mutant V_H-Y100aA showed less extensive association, but a larger k_{obs}, within the same concentration range. Although the smaller signal change gives rise to a larger error, this variant also displayed a linear dependence of k_{obs} on concentration with a slope of 5.7 × 10^4 M^{-1} s^{-1}. As shown in Figure 2A, hu4D5-5 Fab gave a slow rate of dissociation from immobilized antigen. These data were analyzed using the linear rate equation (eq 4) to obtain a value of 1.7 ± 0.3 × 10^{-5} s^{-1} for k_{diss}. As shown in Figure 2B, there are small deviations from linearity for these data, suggesting that dissociation followed by rebinding may occur; nonetheless, the K_D calculated from the kinetic constants compares favorably with the value determined previously from equilibrium measurements (Table I). V_H-Y100aA dissociated too rapidly (Figure 2A) to determine k_{diss} by using eq 4, and thus k_{diss} was determined by extrapolation of the data of Figure 1C.

All of the mutants studied displayed a linear dependence of k_{obs} on concentration, which indicates binding can be described by a single bimolecular association reaction (eq 6) as opposed to a more complicated scheme (eq 7) where a rapid equilibrium step is followed by a slow isomerization to a more stable complex.

$$\mathrm{Ab} + \mathrm{Ag} \underset{k_{diss}}{\overset{k_{assoc}}{\rightleftarrows}} \mathrm{Ab\text{–}Ag} \qquad (6)$$

$$\mathrm{Ab} + \mathrm{Ag} \underset{k_{-1}}{\overset{k_1}{\rightleftarrows}} \mathrm{Ab\text{–}Ag} \underset{k_{-2}}{\overset{k_2}{\rightleftarrows}} \mathrm{Ab\text{–}Ag^*} \qquad (7)$$

For mechanism 7 the pseudo-first-order rate constant will have a nonlinear dependence on antibody concentration (Järv et al., 1979). Although the limited concentration range (10

Table I: Kinetics and Equilibria of hu4D5 Fab Binding to Immobilized p185$^{HER2-ECD}$ [a]

mutant	$k_{assoc} \times 10^{-4}$ (M^{-1} s^{-1})	$k_{diss} \times 10^{5}$ (s^{-1})	K_D (nM)	ΔH (kcal mol^{-1})
hu4D5-5 (WT)	6.4 ± 0.9	1.7 ± 0.3	0.27 ± 0.06 (0.43 ± 0.12)	−10.4 ± 0.6
V_L-D28N	7.5	1.3	0.17	−8.7
V_L-N30A	4.1	7.2	1.75	ND[b]
V_L-T31A	6.5	6.7	1.04	−7.1
V_L-Y49A	5.9	9.7	1.60	−9.5
V_L-S50A	7.3	1.7	0.24	−9.8
V_L-S52A	10.4	1.6	0.16	−12.3
V_L-F53N	3.2	6.5	2.02	−8.7
V_L-E55Y	7.4	1.5	0.20 (0.16)	−11.3
V_L-R66G	6.5	2.5	0.39 (1.10)	−8.6
V_L-H91A	3.2	170	55.0	−10.0
V_L-H91F	6.7	0.9	0.13	−15.4
V_L-Y92A	4.1	11.0	2.70	−8.2
V_L-Y92F	7.5	1.4	0.19	−10.6
V_L-T93A	4.3	4.7	1.10	−9.6
V_L-T94A	6.6	1.5	0.22	−9.8
V_H-K30A	2.9	2.1	0.74	−9.1
V_H-D31A	3.6	1.5	0.41	−10.1
V_H-T32A	3.8	1.9	0.51	−8.9
V_H-Y33A	8.0	1.8	0.23	−11.7
V_H-R50A	3.5	2100	610	−7.2
V_H-Y52A	4.3	1.7	0.40	−11.7
V_H-T53A	4.9	1.5	0.31	−9.5
V_H-N54A	8.6	1.8	0.21	−10.6
V_H-Y56A	4.1	4.9	1.18	−9.2
V_H-W95A	3.9	19000	5000 [1400]	−8.3
V_H-D98A	2.0	4.3	2.15	−7.5
V_H-F100A	4.7	9.0	1.9	−12.5
V_H-Y100aA	5.7	19000	3400 [340]	−6.8
V_H-Y100aF	16.1	3.9	0.25	−8.9
V_L-H91A:V_H-Y100aA	0.06	490	8800	−4.3
V_H-W95A:V_H-Y100aA	0.03	185	6300	0[c]

[a] Values shown for hu4D5-5 (wild-type) represent the mean ± standard deviation of triplicate measurements. The values shown for the mutant proteins represent single determinations with the standard error assumed to be similar to that observed for the wild-type protein. Numbers in parentheses and brackets are K_D values determined by using a radioimmunoassay (Kelley et al., 1992) or by using titration calorimetry (Wiseman et al., 1989), respectively, indicating mostly good agreement with the values determined by the kinetics method. V_L-E55Y and V_L-R66G are replacements of framework residues shown previously to be important for antigen binding (Kelley et al., 1992). [b] ND = not determined. [c] No heat of binding was detected for this variant by using 10 μM p185$^{HER2-ECD}$.

nM to 1.3 μM) accessible to SPR measurements makes it difficult to completely exclude mechanism 7, the good agreement in K_D values obtained by SPR or RIA (Table I) suggests that mechanism 6 is sufficient to describe the data. For mutants with fast off-rates (i.e., V_H-W95A and V_H-Y100aA) k_{diss} must be determined by extrapolation of the concentration dependence of k_{obs}, with a concomitant larger error, and thus the agreement in K_D values between the equilibrium (calorimetry) and kinetic methods is less favorable.

As shown in Table I, changes in affinity result primarily from effects on the rate of dissociation as was previously observed for the variation in affinity of anti-hapten antibodies (Pecht, 1982). Recently, Northrup and Erickson (1992) have used a Brownian dynamics simulation method to model the rates of protein–protein association reactions in solution. These rates are generally much faster than would be predicted on the basis of geometric considerations. The Brownian dynamics simulation can accurately model the rate of protein–protein association with the rate enhancement over the geometric rate constant attributed to a diffusive entrapment effect involving multiple collisions per protein–protein encounter. Single amino acid substitutions presumably have little effect on this diffusion entrapment effect. In contrast, combining two single mutations that individually have large effects on k_{diss}, but only small effects on k_{assoc}, results in a Fab with a very small association rate constant (Table I).

The Functional Epitope of hu4D5-5. Four mutations, V_L-H91A, V_H-R50A, V_H-W95A, and V_H-Y100aA, result in greater than 200-fold decreases in affinity ($\Delta\Delta G$ > 3 kcal mol^{-1}; Figure 3), six mutations, V_L-N30A, V_L-Y49A, V_L-F53N, V_L-Y92A, V_H-D98A, and V_H-F100A, manifest 1–2 kcal mol^{-1} $\Delta\Delta G$ values, and the remaining 17 mutants have small or negligible effects on binding ($|\Delta\Delta G|$ = 0–1 kcal mol^{-1}). A set of four mutations, all in V_L (D28N, S52A, H91F, and Y92F), result in small but significant increases in affinity ($\Delta\Delta G$ = −0.2 to −0.4 kcal mol^{-1}). These data are consistent with results of free energy calculations on lysozyme–antibody complexes (Novotny et al., 1989) which suggest that only a few of the contacts observed by X-ray crystallography (Davies et al., 1990) dominate the energetics of antigen binding. Similar results have been observed for the variation in antibody affinity with mutations in antigen residues for anti-human growth hormone antibodies (Jin et al., 1992) and an anti-neuraminidase antibody (Nuss et al., 1993).

The X-ray structure of hu4D5 Fv (Eigenbrot et al., 1993) shows that all four of the critical antigen binding residues line a shallow depression on the surface of the antibody (Figure 4) and thus define a putative antigen binding pocket. Unlike the other mutations described here, these four sites do not display enthalpy–entropy compensation (Lumry & Rajender, 1970; Eftink et al., 1983) as $\Delta\Delta G$ is larger than $\Delta\Delta H$. Solvent accessibility calculations (Lee & Richards, 1971; Table II) indicate that most of the V_H-Y100a side chain but only the polar portion of the V_H-R50 side chain are accessible and thus could directly contact antigen. The solvent accessibility of the V_H-R50 side chain suggests that this residue contributes to binding by forming a salt bridge or hydrogen bond(s) with the antigen. In contrast, most of the V_L-H91 and V_H-W95

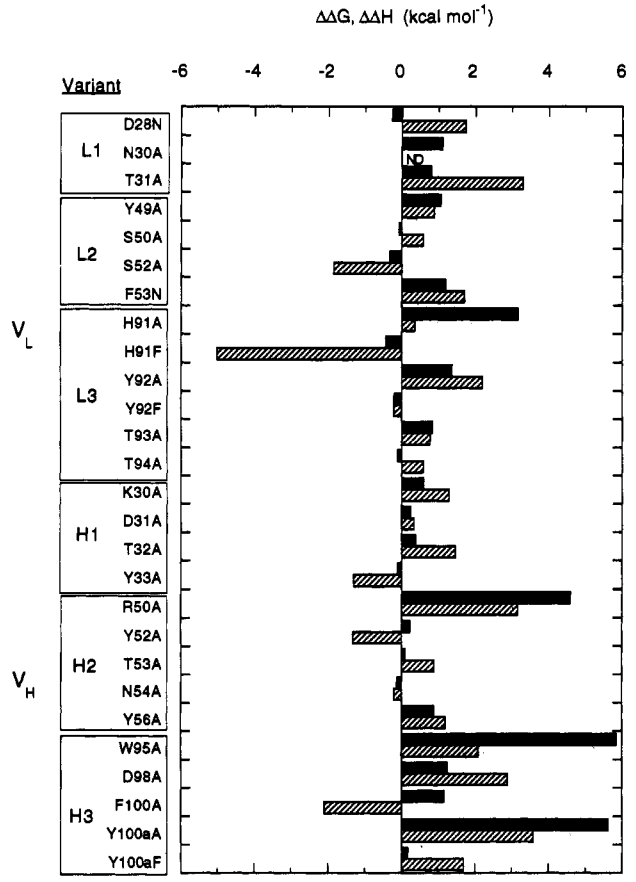

FIGURE 3: Effect of single-site mutations in hu4D5-5 Fab on the thermodynamics of binding to p185$^{HER2-ECD}$. Results are shown as $\Delta\Delta J$ values ($J = G$ or H), where $\Delta\Delta J = \Delta J_{mut} - \Delta J_{WT}$. $\Delta G° = -RT \ln(1/K_D) = \Delta H - T\Delta S°$; the standard state is unit molarity. $\Delta\Delta G$ values are shown as solid bars and $\Delta\Delta H$ values as slashed bars. ND = not determined. Each box denotes a CDR segment from the light (L1, L2, L3) or heavy (H1, H2, H3) chain.

side chains are buried and thus may have indirect roles in antigen binding by maintaining the structure of the antigen binding site. A Phe residue at site V_L-91 was expected to preserve this structure, and thus the V_L-H91F mutant retains good antigen affinity. The V_L-H91F mutant displays a large and negative $\Delta\Delta H$ which may indicate that the V_L-H91 side chain must be deprotonated at pH 7.5, an endothermic process, prior to binding. For this suggestion to be correct, V_L-H91 must have an abnormal pK_a of greater than 7.5. Both V_L-H91 and V_H-W95 make nonadditive (Wells, 1990) contributions to antigen binding with V_H-Y100a as shown by examining the functional properties of the double mutants V_L-H91A:V_H-Y100aA and V_H-W95A:V_H-Y100aA (Table I). These data indicate that for residues displaying large $\Delta\Delta G$ values the assignment of the thermodynamic effect to the wild-type side chain is difficult because a mutation at one site may perturb the role of an adjacent site within the pocket.

Residues in the intermediate functional class ($\Delta\Delta G$ = 1–2 kcal mol^{-1}) are arranged about the periphery of the putative antigen binding pocket, and except for V_H-F100, the data indicate that these residues contribute to binding through a favorable ΔH compensated by an unfavorable ΔS, most noticeable for V_H-D98. Part of the unfavorable ΔS may result because these side chains are on the antibody surface and thus mobile but become fixed upon antigen binding (Novotny et al., 1989). Similarly, most of the sites that have $|\Delta\Delta G|$ = 0–1 kcal mol^{-1} also have $\Delta\Delta H > \Delta\Delta G$, suggesting that the side chain does contact antigen but does not contribute a favorable interaction to binding. These results are consistent with known structures of antibody–antigen complexes which show that 14–21 antibody residues are in van der Waals contact with protein antigen (Davies et al., 1990).

Role of Polar and Nonpolar Interactions in Antigen Binding. Although the lack of a structure for the antibody–antigen complex precludes a rigorous interpretation, some preliminary predictions about the role of certain residues can be made on the basis of $\Delta\Delta C_p$ values. The mutations V_L-Y92A, V_H-R50A, V_H-W95A, and V_H-Y100aA result in positive $\Delta\Delta C_p$ values (Table II) that are greater than the uncertainty in the measurements (±40 cal mol^{-1} K^{-1}), indicating that these substitutions weaken the contribution to binding from the hydrophobic effect. All of these mutations result in weaker antigen binding, thus highlighting the importance of the hydrophobic effect for driving the interaction. These substitutions, except for V_H-R50A, replace a large nonpolar residue with a smaller side chain, and thus the sign of $\Delta\Delta C_p$ is consistent with the model compound data (Gill et al., 1976; Murphy & Gill, 1991). Since the side chains of both V_H-R50 and V_H-W95 have very little solvent-accessible nonpolar surface in the free antibody (Table II), the V_H-R50A and V_H-W95A mutations probably indirectly weaken the contribution to binding from the hydrophobic effect. The V_H-W95A mutation probably alters the structure of the binding site since the W side chain is buried and seems to anchor CDR H3 to the surface of the antibody. Loss of a salt bridge and/or hydrogen bonds with V_H-R50 may prevent proper docking of antigen in the pocket, thus weakening the hydrophobic contribution from other sites within the pocket.

As expected for a decrease in burial of polar residues in the interface with antigen, negative $\Delta\Delta C_p$ values are observed for V_L mutations D28N and Y92F and V_H mutations T32A, Y33A, Y52A, and Y100aF. All of these mutations have small $\Delta\Delta G$ values, indicating that polar interactions do not provide a large driving force for antigen binding. The V_H substitution F100A has an unexpected negative $\Delta\Delta C_p$ value. V_H100 is an interdomain contact residue (Chothia et al., 1985; Eigenbrot et al., 1993), and thus the Ala substitution probably affects V_H/V_L association.

Thermodynamic Contributions from Antibody Tyr Residues. The effect of Phe substitutions at sites V_L-Y92 and V_H-Y100a indicates that the side-chain hydroxyls of these residues do not contribute to the free energy of antigen binding. These substitutions result in negative $\Delta\Delta C_p$ values (Table II), suggesting that the side-chain hydroxyls may become buried in the interface with antigen. The V_H-Y100aF mutant has a $\Delta\Delta H$ value of −1.5 kcal mol^{-1}, which might indicate a change in the hydrogen bonding of the Y side-chain hydroxyl upon binding to antigen. This group appears to be hydrogen bonded to V_H-D98 in the X-ray structure of the free Fv fragment (Eigenbrot et al., 1993; Figure 4), and thus the $\Delta\Delta H$ effect might also be related to incorrect positioning of the V_H-D98 side chain.

Since both the V_L-Y92F and V_H-Y100aF mutations have negligible $\Delta\Delta G$ values, the effects of Ala replacements at these sites must be related to the contributions from the aromatic ring to antigen binding. Both V_L-Y92A and V_H-Y100aA mutants have positive $\Delta\Delta C_p$ values, which is consistent with a contribution to ΔG from the hydrophobic effect through burial of the aromatic ring in the interface with antigen. These Y side chains have considerable solvent-accessible nonpolar surface available for antigen binding as shown in Table II. In contrast, the V_H mutations Y33A and Y52A have negative $\Delta\Delta C_p$ values as expected for a decrease in polar interactions. More of the aromatic ring of these two

Table II: Effect of Amino Acid Substitutions on the ΔC_p for Antigen Binding[a]

variant	ΔG (kcal mol^{-1})	$\Delta\Delta G$ (kcal mol^{-1})	ΔC_p (cal mol^{-1} K^{-1})	$\Delta\Delta C_p$ (cal mol^{-1} K^{-1})	A_p[b] (Å^2)	A_{np} (Å^2)
hu4D5-5 (WT)	−13.1 ± 0.15		−320 ± 20			
V_L-D28N	−13.4	−0.3	−400	−80	34.6	39.5
V_L-Y92F	−13.3	−0.2	−380	−60	48.0	39.6
V_H-T32A	−12.7	+0.4	−430	−110	0.0	6.7
V_H-Y33A	−13.2	−0.1	−400	−80	33.2	20.2
V_H-Y52A	−12.9	+0.2	−450	−130	39.4	17.6
V_H-F100A	−11.9	+1.2	−400	−80	0.0	41.4
V_H-Y100aF	−13.1	0.0	−380	−60	26.6	58.9
V_L-H91A	−9.9	+3.2	−270	+50	1.6	8.8
V_L-Y92A	−11.7	+1.4	−240	+80	48.0	39.6
V_H-R50A	−8.5	+4.6	−200	+120	33.6	0.0
V_H-W95A	−7.3	+5.9	−210	+110	0.0	20.4
V_H-Y100aA	−7.5	+5.6	−250	+70	26.6	58.9

[a] For the mutant proteins, enthalpy measurements were made at 25 and 37 °C in order to determine ΔC_p. $\Delta\Delta C_p = \Delta C_{p(mut)} - \Delta C_{p(WT)}$. The uncertainty in $\Delta\Delta C_p$ is estimated to be ±40 cal mol^{-1} K^{-1}. [b] The solvent-accessible surface area of the wild-type side chain was calculated from the X-ray structure of hu4D5 Fv (Eigenbrot et al., 1993) as described by Lee and Richards (1971) by using a probe of 1.4-Å radius. This surface area was divided into polar (A_p) and nonpolar (A_{np}) contributions.

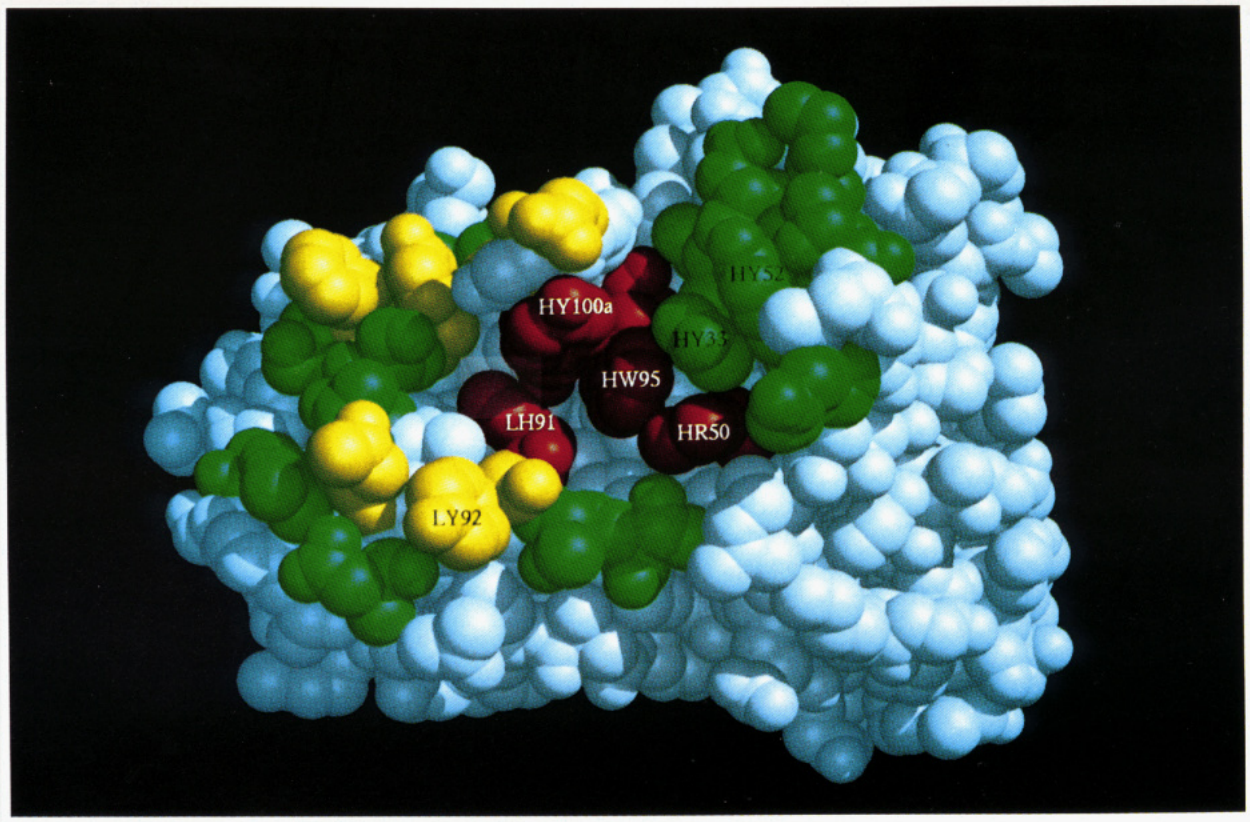

FIGURE 4: Antigen binding surface of hu4D5. A space-filling model of the structure of hu4D5 Fv determined at 2.2 Å (Eigenbrot et al., 1993) is shown looking down on the CDR loops with the light chain on the left. A few side chains are labeled, with the first letter denoting light (L) or heavy (H) chain. Side chains are colored according to the magnitude of the effect of the alanine substitution on the ΔG for antigen binding: red = >3 kcal mol^{-1} $\Delta\Delta G$, yellow = 1–2 kcal mol^{-1} $\Delta\Delta G$, green = 0–1 kcal mol^{-1} $\Delta\Delta G$, and white = untested.

side chains is buried in the free Fv fragment while the hydroxyl is accessible to solvent and thus could make a hydrogen bond with antigen. These putative hydrogen bonds would be weaker than the ones formed with water in the free antibody as shown by the sign of $\Delta\Delta H$. Clearly, these predictions based on thermodynamic data require confirmation through structure determination of the antibody–antigen complex.

The large $\Delta\Delta G$ value of the V_H-Y100aA mutant, as well as the observation of nonadditive effects of this mutation with the V_L-H91A and V_H-W95A changes (Table I), suggests that this substitution may perturb the contributions from other side chains. The smaller $\Delta\Delta G$ value for the V_L-Y92A mutant suggests that this substitution does not significantly perturb the binding site structure and that the contribution of the V_L-Y92 side chain may be considered independent of other interactions. Thermodynamic parameters for burial of the phenyl ring may be calculated from the data on the V_L-Y92A and V_L-Y92F mutants. As shown in Table III, burial of the V_L-Y92 aromatic ring is enthalpy driven at 25 °C and opposed by ΔS. This latter feature is inconsistent with the liquid hydrocarbon (Baldwin, 1986) and solid dissolution (Murphy & Gill, 1991) models of the hydrophobic effect. In addition, although the calculated ΔG and ΔH values are similar to those obtained from the thermodynamics of solid compound dissolution in water, the ΔC_p is too large. Indeed, we calculate a burial of 480 Å^2 of nonpolar surface area from ΔC_p by using an area-normalized heat capacity change of 0.27 cal mol^{-1} K^{-1} Å^{-2} (Connelly & Thomson, 1992). A similar study of S-peptide variants binding to S-protein detected an even larger disparity between ΔC_p and ΔA_{np} (Varadarajan et al., 1992).

Table III: Thermodynamic Parameters for Burying a Solvent-Accessible Phenyl Group[a]

method	ΔG	ΔH	ΔS	ΔC_p
V_L-Y92[b]	−1.6	−2.4	−2.8	−140
V_H-Y100a[c]	−4.3	−2.1	+7.0	−130
solid[d]	−1.1	−1.6	+0.5	−31
liquid[e]	−3.9	−0.5	+13	−53

[a] Units of ΔG and ΔH are kcal mol^{-1}; ΔS and ΔC_p are in cal mol^{-1} K^{-1}. [b] Observed difference in antigen binding thermodynamics between V_L-Y92F and V_L-Y92A mutants. [c] Observed difference in antigen binding thermodynamics between V_H-Y100aF and V_H-Y100aA mutants. For the ΔG calculation the binding constant obtained for V_H-Y100aA from calorimetry was used. [d] Calculated from thermodynamic data on the dissolution of solid compounds in water (Murphy & Gill, 1991). [e] Calculated from thermodynamic data on the transfer of liquid hydrocarbons to water (Gill et al., 1976).

Part of this discrepancy may result because the mutational data includes a contribution from the loss of V_L-Y92 sidechain rotational freedom upon antigen binding. Mutation may also perturb the changes in low-energy vibrational modes that accompany binding. Both of these effects are expected to yield negative values for ΔS and ΔC_p (Sturtevant, 1977). Substitution of V_L-Y92 with Ala might result in a cavity in the interface with antigen, or a slight repacking of the interface, which could have significant energetic consequences (Eriksson et al., 1992). This analysis highlights the difficulty, also noted by others (Connelly et al., 1991; Varadarajan et al., 1992), of correlating the thermodynamic effects of mutations with model compound data and also with the structures of the components.

Suzuki et al. (1992) have recently reported experimental evidence for the formation of weak hydrogen bonds between water and the π-electron cloud of the benzene ring. This result suggests that there could be weak hydrogen bonds between water and solvent-accessible aromatic rings in the free antibody that are replaced by aromatic–aromatic or aromatic–amide interactions (Levitt & Perutz, 1988) in the complex. Part of the exothermic ΔH calculated for the phenyl group contribution to antigen binding (Table III) might reflect re-formation of water–water hydrogen bonds. Given the high occurrence of Tyr residues in antibody CDR loops (Padlan, 1990), a significant portion of the ΔH of antigen binding might result from this process.

Despite the limitations noted above, the thermodynamic parameters extracted from analysis of the V_L-Y92 mutants predict that phenyl groups should have a minimum solubility in water at 10 °C, where $\Delta H = 0$, consistent with the known temperature dependence of benzene solubility (Gill et al., 1976). In addition, the ΔG contribution from burial of the phenyl group in the interface with antigen will have a maximum at 20 °C, where $\Delta S = 0$. Most native proteins display a similar temperature of maximum stability (Privalov & Khechinashvili, 1974) with the driving force for folding attributed to the hydrophobic effect (Kauzmann, 1959). Our analysis indicates that the contribution from aromatic side chains to ΔG is strongest near ambient temperature.

In conclusion, we find that the driving force for antigen binding is provided by the hydrophobic effect and also a potential salt bridge or hydrogen bond(s) with V_H-R50. Sidechain hydrogen bonds do not appear to play a prominent role in antigen binding. Discrimination between closely related antigens must arise from complementarity of the antigen to the hydrophobic pocket on the antibody and also a lack of steric conflicts as shown by the small number of mutations that result in increased affinity. Antibody Tyr residues make favorable contributions to binding by burial of the aromatic ring in the interface with antigen. This process has features (i.e., $\Delta S < 0$) that are not completely consistent with the current models of the hydrophobic effect. Selection of Tyr as opposed to Phe for this purpose may reflect the need to maintain solubility of the free antibody.

ACKNOWLEDGMENT

We thank Drs. Len Presta, Paul Carter, and Charles Eigenbrot for many helpful and stimulating discussions. We also thank Dr. Brad Snedecor and Mr. Mike Covarrubias for fermentation support. We are grateful to Dr. David Vetterlein and Mr. Riley Spreckart for supplying purified p185$^{HER2-ECD}$. We thank Drs. Tony Kossiakoff, Robert Lazarus, Jeff Livingstone, Jim Wells, Fred Richards, Julian Sturtevant, and Jiri Novotny for critical review of the manuscript.

REFERENCES

Baldwin, R. L. (1986) *Proc. Natl. Acad. Sci. U.S.A. 83*, 8069–8072.

Carter, P., Kelley, R. F., Rodrigues, M. L., Snedecor, B., Covarrubias, M., Velligan, M. D., Wong, W.-L. T., Rowland, A. M., Kotts, C., Carver, M. E., Yang, M., Bourell, J. H., Shepard, H. M., & Henner, D. (1992a) *Bio/Technology 10*, 163–167.

Carter, P., Presta, L., Gorman, C. M., Ridgway, J. B. B., Henner, D., Wong, W.-L. T., Rowland, A. M., Kotts, C., Carver, M. E., & Shepard, H. M. (1992b) *Proc. Natl. Acad. Sci. U.S.A. 89*, 4285–4289.

Chothia, C., Novotny, J., Bruccoleri, R., & Karplus, M. (1985) *J. Mol. Biol. 186*, 651–663.

Connelly, P., Ghosaini, L., Hu, C.-Q., Kitamura, S., Tanaka, A., & Sturtevant, J. M. (1991) *Biochemistry 30*, 1887–1891.

Connelly, P. R., & Thomson, J. A. (1992) *Proc. Natl. Acad. Sci. U.S.A. 89*, 4781–4785.

Cunningham, B. C., & Wells, J. A. (1989) *Science 244*, 1081–1085.

Davies, D. R., Padlan, E. A., & Sheriff, S. (1990) *Annu. Rev. Biochem. 59*, 439–473.

Eftink, M. R., Anusiem, A. C., & Biltonen, R. L. (1983) *Biochemistry 22*, 3884–3896.

Eigenbrot, C., Randal, M., Presta, L., Carter, P., & Kossiakoff, A. A. (1993) *J. Mol. Biol. 229*, 969–995.

Eriksson, A. E., Baase, W. A., Zhang, X.-J., Heinz, D. W., Blaber, M., Baldwin, E. P., & Matthews, B. W. (1992) *Science 255*, 178–183.

Fendly, B. M., Kotts, C., Vetterlein, D., Lewis, G. D., Winget, M., Carver, M. E., Watson, S. R., Sarup, J., Saks, S., Ullrich, A., & Shepard, H. M. (1990) *J. Biol. Response Modif. 9*, 449–455.

Gill, S. J., Nichols, N. F., & Wadsö, I. (1976) *J. Chem. Thermodyn. 8*, 445–452.

Hudziak, R. M., Lewis, G. D., Winget, M., Fendly, B. M., Shepard, H. M., & Ullrich, A. (1989) *Mol. Cell. Biol. 9*, 1165–1172.

Järv, J., Hedlund, B., & Bartfai, T. (1979) *J. Biol. Chem. 254*, 5595–5598.

Jin, L., Fendly, B. M., & Wells, J. A. (1992) *J. Mol. Biol. 226*, 851–865.

Kabat, E. A., Wu, T. T., Perry, H. M., Gottesman, K. S., & Foeller, C. (1991) *Sequences of Proteins of Immunological Interest*, 5th ed., National Institutes of Health, Washington, DC.

Karlsson, R., Michaelsson, A., & Mattsson, L. (1991) *J. Immunol. Methods 145*, 229–240.

Kauzmann, W. (1959) *Adv. Protein Chem. 14*, 1–63.

Kelley, R. F., O'Connell, M. P., Carter, P., Presta, L., Eigenbrot, C., Covarrubias, M., Snedecor, B., Bourell, J. H., & Vetterlein, D. (1992) *Biochemistry 31,* 5434–5441.
Langerman, N., & Biltonen, R. L. (1979) *Methods Enzymol. 61,* 261–286.
Lee, B., & Richards, F. M. (1971) *J. Mol. Biol. 55,* 379–400.
Levitt, M., & Perutz, M. F. (1988) *J. Mol. Biol. 201,* 751–754.
Lumry, R., & Rajender, S. (1970) *Biopolymers 9,* 1125–1227.
Murphy, K. P., & Gill, S. J. (1991) *J. Mol. Biol. 222,* 699–709.
Northrup, S. H., & Erickson, H. P. (1992) *Proc. Natl. Acad. Sci. U.S.A. 89,* 3338–3342.
Novotny, J., Bruccoleri, R. E., & Saul, F. A. (1989) *Biochemistry 28,* 4735–4749.
Nuss, J. M., Whitaker, P. B., & Air, G. M. (1993) *Proteins: Struct., Funct., Genet. 15,* 121–132.
Padlan, E. A. (1990) *Proteins: Struct., Funct., Genet. 7,* 112–124.
Pecht, I. (1982) *Antigens 6,* 1–68.
Privalov, P. L., & Khechinashvili, N. N. (1974) *J. Mol. Biol. 86,* 665–684.
Riechmann, L., Clark, M., Waldmann, H., & Winter, G. (1988) *Nature (London) 332,* 323–327.
Sturtevant, J. M. (1977) *Proc. Natl. Acad. Sci. U.S.A. 74,* 2236–2240.
Suzuki, S., Green, P. G., Bumgarner, R. E., Dasgupta, S., Goddard, W. A., & Blake, G. A. (1992) *Science 257,* 942–945.
Tanford, C. (1980) in *The Hydrophobic Effect,* John Wiley & Sons, New York.
Varadarajan, R., Connelly, P. R., Sturtevant, J. M., & Richards, F. M. (1992) *Biochemistry 31,* 1421–1426.
Wells, J. A. (1990) *Biochemistry 29,* 8509–8517.
Wells, J. A., Vasser, M., & Powers, D. B. (1985) *Gene 34,* 315–323.
Wiseman, T., Williston, S., Brandts, J. F., & Lin, L.-N. (1989) *Anal. Biochem. 179,* 131–137.